FOREWORD

This program was conducted by the National Carbon Company, a Division of Union Carbide Corporation, under USAF Contract AF 33(616)-6915. This contract was initiated under Project No. 7350 "Refractory Inorganic Non-Metallic Materials", Task No. 735002 "Refractory Inorganic Non-Metallic Materials: Graphitic"; Project No. 7381 "Materials Application", Task No. 738102 "Materials Process"; and Project No. 7-817 "Process Development for Graphite Materials". The work was administrated under the direction of the Air Force Materials Laboratory, Research and Technology Division, with Captain R. H. Wilson, L. J. Conlon and W. P. Conrardy acting as Project Engineers.

The work covered in this report was performed by Union Carbide European Research Associates at Brussels, Belgium under subcontract to National Carbon Company during the period January 1, 1962 through December 31, 1962.

Other reports issued under USAF Contract Af 33(616)-6915 have included:

WADD technical Notes 61-18 and 61-18, Part II, progress reports covering work from the start of the Contract on May 1, 1960 to October 15, 1961, and the following volumes of WADD Technical Report 61-72 covering various subject phases of the work:

Volume I	Observations by Electron Microscopy of Dislocations in Graphite, by R. Sprague.
Volume II	Applications of Anisotropic Elastic Continuum Theory to Dislocations in Graphite, by G. B. Spence.
Volume III	Decoration of Dislocations and Low Angle Grain Boundaries in Graphite Single Crystals, by R. Bacon and R. Sprague.
Volume IV	Adaptation of Radiographic Principles to the Quality Control of Graphite, by R. W. Wallouch.
Volume V	Analysis of Creep and Recovery Curves for ATJ Graphite, by E. J. Seldin and R. N. Draper.
Volume VI	Creep of Carbons and Graphites in Flexure at High Temperatures, by E. J. Seldin.
Volume VII	High Density Recrystallized Graphite by Hot Forming, by E. A. Neel, A. A. Kellar, and K. J. Zeitsch.
Volume VII Supplement	High Density Recrystallized Graphite by Hot Forming, by G. L. Rowe and M. B. Carter.
Volume VIII	Electron Spin Resonance in Polycrystalline Graphite, by L. S. Singer and G. Wagoner.

Volume IX	Fabrication and Properties of Carbonized Cloth Composites, by W. C. Beasley and E. L. Piper.
Volume X	Thermal Reactivity of Aromatic Hydrocarbons, by I. C. Lewis and T. Edstrom.
Volume X Supplement	Thermal Reactivity of Aromatic Hydrocarbons, by I. C. Lewis and T. Edstrom.
Volume XI	Characterization of Binders Used in the Fabrication of Graphite Bodies, by E. de Ruiter, A. Halleux, V. Sandor, H. Tschamler.

ABSTRACT

A typical coal tar pitch has been separated into fractions which have been analyzed and characterized by selected physical and chemical methods. These results have indicated the presence of molecules consisting of from one to several aromatic clusters, each having a mean cluster size near four aromatic rings. Information has been obtained on aromaticity, hydrogen distribution and substitution index.

A study has been made of the effect of temperature and different atmospheres on the plasticity of the various fractions of the pitch sample.

This report has been reviewed and is approved.

W. G. RAMKE
Chief, Ceramics and Graphite Branch
Metals and Ceramics Division
AF Materials Laboratory

TABLE OF CONTENTS

LIST OF ILLUSTRATIONS

1. INTRODUCTION

An earlier report[1], WADD Technical Report 61-72, Volume XI, described the definition of structural parameters for thirteen selected samples of tars and pitches of interest in the fabrication of graphite bodies employing chemical and physical methods previously used in the study of the constitution of coals.

Pitches were shown to be complex mixtures of highly aromatic molecular species, which can be classified into three groups of compounds having:

a) a low molecular weight (< 300)
b) a medium molecular weight (300-1200)
c) a high molecular weight (< 1200).

Each group will show different behavior on thermal treatment. Whereas compounds of group a) may evaporate, polymerize, or decompose at relatively low temperatures, the material of high molecular weight can be assumed to be unreactive. Substances belonging to group b) are more stable than those of group a) but much more reactive than the molecular species of group c) and may, therefore, influence the binder quality of a pitch.

Subsequent work has been concentrated on a sample of 30-medium pitch (Pitch No. 5 from previous report[1]) for which characteristic data are summarized in Table 1. Our investigations have been mainly concerned with the separation of the pitch into fractions with respect to molecular weight. Furthermore, a structural analysis has been undertaken on several of the fractions obtained. Finally, the plastic behavior of some of the fractions has been determined.

Table 1. Analytical Data and Some Properties of Pitch No. 5

% C	92.9	Softening Point (°C)	99 *
% H	4.2	C.V. (%)	60.7*
% O	1.2		
% N	0.7	Pyridine insoluble (%)	21
% S (diff)	1.0	Benzene insoluble (%)	33
		d^{25}_{He}	
% VM	60.2		1.317
		$d^{25}_{H_2O}$	
% ash	0.23		1.321
		$\bar{M}$ (Hill Baldes)	330

* as reported by National Carbon Company.

Manuscript released by the authors November 1963 for publication as an ASD Technical Documentary Report.

2. SUMMARY

Pitch is a complicated mixture of various types of molecules, the behavior of which during carbonization will not depend only on their chemical structure but also on their size. Small molecules can evaporate before they are able to react, while the very large cross-linked molecules, as a result of their rigidity, may be quite unreactive. Since all types of molecules in pitch are highly aromatic with only a few functional groups, fundamental differences in chemical structure are hardly to be expected, so that the molecular size distribution is thought to be an important factor for the behavior of a pitch during carbonization.

To prove this idea, a 30-medium coal tar pitch (Sample No. 5 of previous report[1]) was separated into a number of less complex fractions which have been investigated by methods of structural analysis.

The pitch was first extracted with benzene. The benzene soluble part (67 per cent) was split into a pet. ether soluble (γ)-fraction (23 per cent) and a pet. ether insoluble (β)-fraction (44 per cent). The benzene insoluble residue (α-fraction, 33 per cent) has been further extracted by pyridine and a pyridine insoluble residue (α_3-fraction, 25 per cent) and a pyridine soluble, benzene insoluble fraction ($\alpha_1 + \alpha_2$; 8 per cent) have been obtained.

As regards the pet. either soluble (γ)-fraction, more than 60 per cent of the material has been identified: there are mainly pure aromatic systems with one cluster per molecule and a mean cluster size of 4-5 aromatic rings. Such systems have limited reactivity and will probably evaporate before reaction can occur. Their presence is, however, necessary to render the pitch sufficiently fluid.

The pet. ether insoluble, benzene soluble (β)-fraction was split into 17 subfractions and a very surprising result was found: molecular weights are either ~ 1100, ~ 600, or ~ 300. Structural parameters derived from physical properties and spectroscopic data strongly indicate the presence of more than one aromatic cluster per molecule in the case of $\bar{M}$ ~ 1100 and 600, the mean cluster size being ~ 5 aromatic rings for all subfractions. Since the β-fraction is less volatile than the γ-fraction, it will not evaporate to a significant extent during carbonization. Furthermore, since the molecules are not cross-linked, they may act as a lubricant up to rather high temperatures, favoring molecular rearrangements. Thus, it is thought that the β-fraction is of high importance for the quality of the pitch.

The pyridine insoluble residue (α_3-fraction) consists certainly of large cross-linked aromatic systems. Since such rigid structures are usually very unreactive, the α_3-fraction has questionable utility in the use of pitch as a binder.

The pyridine soluble, benzene insoluble ($(\alpha_1 + \alpha_2)$-)fraction was little investigated. It represents only 8 per cent of the pitch and should be comparable to the β-fraction.

J. C. Pariaud[2], although using another separation method, split pitches into three parts, which are quite comparable to our γ-, β- and α-fraction. Pariaud found empirically that it is desirable that the highly insoluble material should not increase during carbonization up to 400°C, while the medium fractions (comparable to our β-fraction) should increase at the expense of the light fraction (γ-fraction). These results can be understood in the light of our structural investigation from which it is concluded that the fraction with medium molecular weight is the most important one.

Another part of the work deals with the plastic behavior of Pitch No. 5 and some of its fractions. Plasticity (which, in principle, is the same as fluidity or the inverse of viscosity) depends on the structure of a material. Therefore, changes in structure and more especially polymerizations and condensations can be followed by changes in plasticity.

At first, Pitch No. 5 itself was investigated at relatively low temperatures, equal to or somewhat higher than those common during the mixing of pitch and coke. At 165°C, no changes of plasticity have been observed, even under pure oxygen. At 190° and 220°C the plasticity decreases rapidly in air.

The α-fraction and its subfractions α_1, α_2 and α_3 have been investigated up to 550°C. No softening at all could be observed in the case of α_3, but it is significant that the initial softening, the maximum plasticity and the resolidification of α, α_1 and α_2 occur at the same temperatures (~ 385°, ~ 470° and ~ 510°C, respectively).

At temperatures up to 200°C, the loss of volatile material from the benzene soluble extract can produce a decrease of plasticity which is not negligible.

3. EXTRACTION OF PITCH NO. 5

From a great number of preliminary experiments, it was found that a solvent extraction with pyridine or benzene is the most suitable way of starting the progressive separation. Finally, benzene was chosen as the first solvent in the overall procedure because the somewhat higher solubility in pyridine causes technical difficulties in the sharp separation of soluble from insoluble material, in particular, in the course of filtration.

In practice, a 500 g sample of Pitch No. 5 was extracted with 50 liters of benzene at its boiling point under purified nitrogen. The benzene insoluble residue has been further extracted with pyridine. The benzene soluble extract was fractionated by stepwise precipitation with pet. ether (40/60°C). The overall extraction and fractionation scheme is given in the following flow sheet:

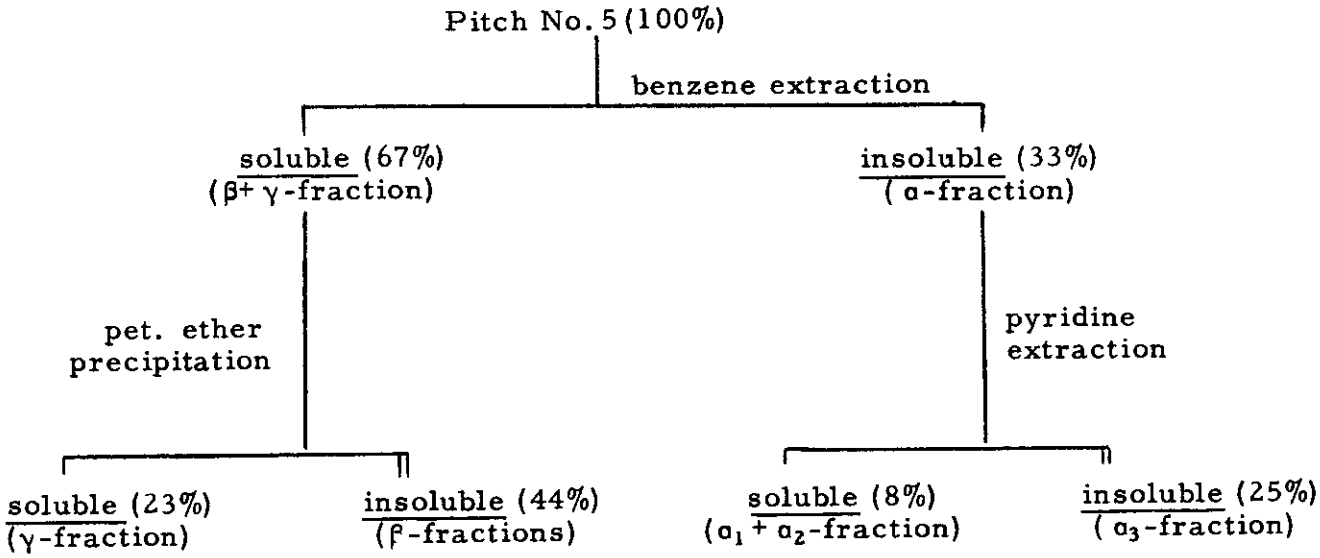

It follows from the solubility characteristics of the fractions finally obtained that approximately 25 per cent of the molecules in Pitch No. 5 possess a relatively low molecular weight (γ-fraction), whereas another 25 per cent (α_3-fraction) consist of species with very high molecular weights. These conclusions have had to be proved and the structural features of the β, α_1 and α_2 fractions carefully investigated, since these fractions represent about 50 per cent of the Pitch No. 5.

Recently J. C. Pariaud has extracted different pitches with pyridine; the extraction was followed by a stepwise precipitation with water [2]. Pariaud found that a certain concentration of water precipated some material (Part A). A further increase in the H_2O concentration had at first no effect; but then after addition of more water, the rest of the material was precipitated (Part B). It can reasonably be assumed that part B is comparable with our γ-fraction and part A with ($\beta + \alpha_1 + \alpha_2$). The presence and the concentration of part A seems to be an important factor for the quality of a pitch as a binder [2].

4. STRUCTURAL INVESTIGATIONS OF THE α-FRACTIONS

There is no doubt that in all these fractions the aromaticity is very high ($C_{ar}/C > 0.95$). In such cases, the absolute value of the atomic ratio H/C is directly related to the size of the aromatic cluster; furthermore, one must know whether the molecules contain only one aromatic cluster or more, in which case the type of the links is also of importance.

The very low H/C value of the α_3-fraction (Table 2) can, therefore, be interpreted either as at least 18 condensed aromatic rings per molecule or a highly cross-linked aromatic system with approximately 10 condensed rings per cluster. Both interpretations are in agreement with i) the low content of volatile matter, ii) the fairly high density, iii) the very low electron activation energy $\Delta\varepsilon$ from electrical conductivity measurements [3], and iv) the fact that the α_3-fraction shows no softening below 550°C (for all parameters, see Table 2).

Table 2. Analytical Data and some Properties of the Benzene Insoluble Residue and of its Subfractions

	Benzene insoluble residue	$(\alpha_1 + \alpha_2)$fraction	α_3-fraction
% C	93.1	91.8	92.7
% H	3.0	4.0	2.7
% O	1.7	1.7	2.1
% $(N+S)_{diff}$	2.2	2.5	2.5
H/C	0.384	0.519	0.347
% VM	13.6	36.4	9.9
% ash	0.8	0.4	0.6
softening pt. (°C)	385 *	310 *	no softening below 550°C
d^{25}_{He}			1.596
$d^{25}_{H_2O}$		1.32	
$\Delta\varepsilon$ (eV)			0.4

* plastometer test.

Under the standardized conditions 4 per cent can be extracted (α_1-fraction) from the benzene insoluble part with pyridine. A further extraction of the residue with fresh pyridine yields another 4 per cent (α_2-fraction). Since α_1 and α_2 together amount only to 8 per cent of Pitch No. 5, these two fractions have been put together.

An inspection of the absolute value of H/C for the (a_1 + a_2) fraction indicates the presence of either a single aromatic cluster with 6-7 condensed rings per molecule. The smaller size of the cluster as compared with that of the a_3-fraction, shows up also in i) the much higher content of volatile matter, ii) the softening point, and iii) the lower density (for these parameters, see Table 2). It can be seen from Table 2 that the data for the a-fraction lie between those of the (a_1 + a_2)- and the a_3-fraction. Since the a_3-fraction represents 76 per cent of the a-fraction, the experimental results of the latter are closer to those of a_3 than of (a_1 + a_2).

5. STRUCTURAL INVESTIGATIONS OF THE γ-FRACTION

This fraction contains the most soluble molecular species of Pitch No. 5 and it is, therefore, reasonable to assume that only one aromatic cluster is present in each molecule. Since aromaticity is certainly very high ($C_{ar}/C > 0.9$), the mean aromatic cluster size ($\bar{R}_{ar}$) can be estimated from the atomic ratio H/C alone and should be 3-4. This statistical result is in agreement with the finding that under nitrogen at 875°C, the γ-fraction evaporates completely (see Table 3, amount of 'volatile matter').

Table 3. Analytical Data and Some Properties of the γ-Fraction

% C	93.6	H_{ar}/H_{al}	4.5
% H	5.3	H_{ar}/H	0.82
% O	1.0	H_{al}/H	0.18
% $(N + S)_{diff}$	1.1	f_a	0.92 ± 0.04
H/C	0.674	S_{ar}	0.40 ± 0.02
% VM	99.2	H_{ar}/C_{ar}	0.635 ± 0.018
% ash	0.0		
$\bar{M}$	305 ± 20		

The UV spectrum of the γ-fraction (Figure 1) supports the above assumptions and conclusions since i) a fairly pronounced structure in the absorption curve can be seen, and ii) the sharp drop in the absorption above ~ 450 mμ is an indication that cluster sizes above 6 can be present only in small amounts.

No conclusions concerning the aromatic cluster sizes can be drawn from the infrared spectrum of the γ-fraction (Figure 1), but some structural information obtained from the positions and intensities of specific bands is worth mentioning:

1) The γ-fraction should consist mainly of aromatic systems which are very little substituted; this conclusion is drawn from the strong aromatic CH-stretching frequency at 3.28 μ (3050 cm^{-1}), from the aromatic HCC-wagging frequencies between 7.5 and 9 μ (1335-1110 cm^{-1}) and especially from the very strong aromatic HCC-rocking frequencies between 10 and 14.5 μ (1000 - 690 cm^{-1}). Substitution by aliphatic groups must be small since the aliphatic CH-stretching band at 3.42 μ (2925 cm^{-1}) is relatively low in intensity.

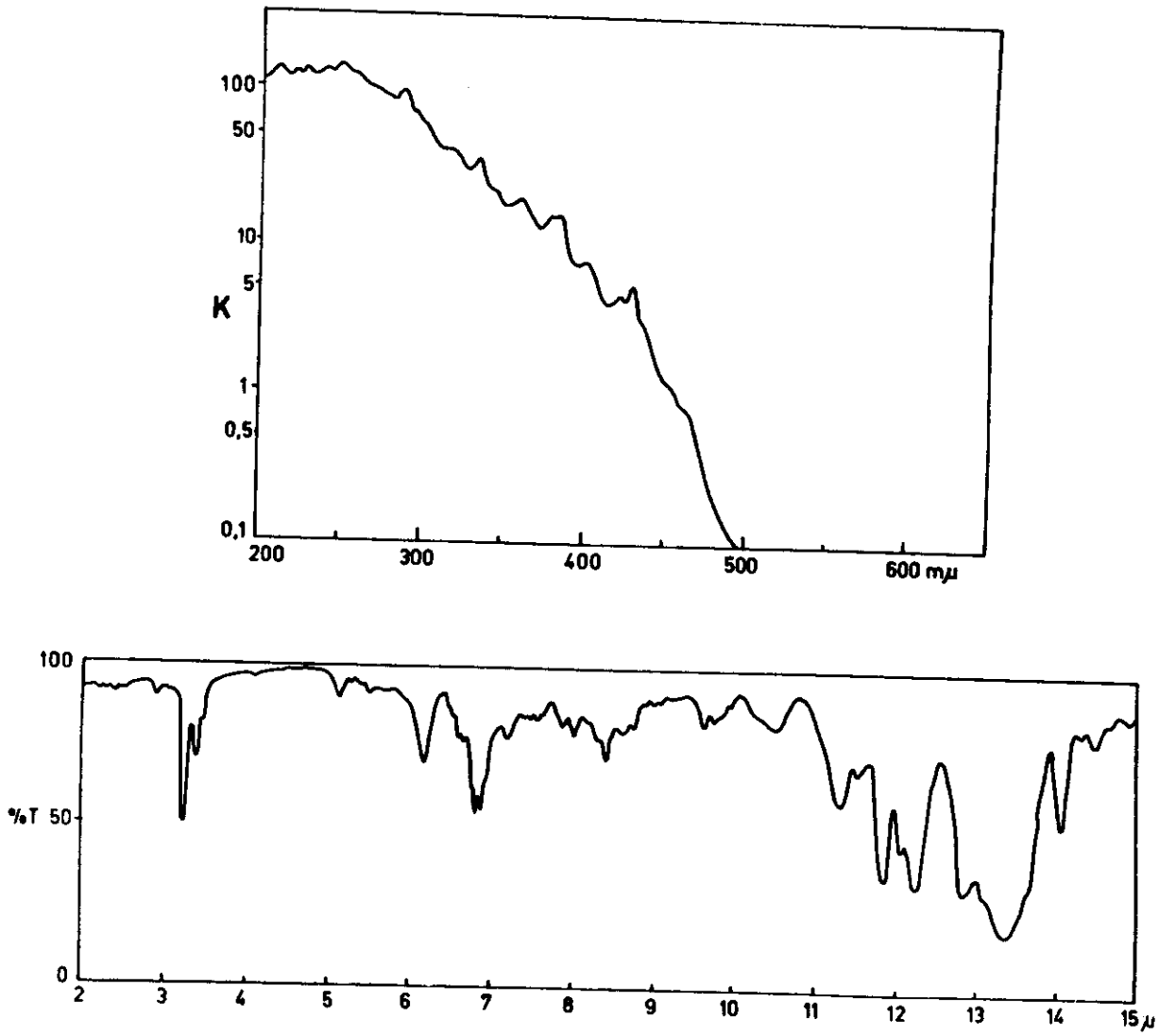

Figure 1. UV-, Visible and Infrared Spectrum of the γ-Fraction

2) From the aromatic and aliphatic CH-stretching bands, the ratio H_{ar}/H_{al} can be calculated [4] and several structural parameters can be derived [5]. Taking into account the fact that the ratio of the maximum extinction coefficients $\varepsilon_{al}/\varepsilon_{ar}$ is 2.0 (see later), H_{ar}/H_{al} can be calculated from the optical densities (D_{ar} and D_{al}) of the aromatic and aliphatic CH-stretching absorptions: [4]

$$\frac{H_{ar}}{H_{al}} = \frac{D_{ar}}{D_{al}} \times \frac{\varepsilon_{al}}{\varepsilon_{ar}} = 2\,\frac{D_{ar}}{D_{al}} \quad .$$

The result is $H_{ar}/H_{al} = 4.5$ and therefore leads to $H_{ar}/H = 0.82$ and $H_{al}/H = 0.18$. With these values, the limits for the aromaticity f_a can be calculated: [5]

$$\frac{C_{ar}}{C} = f_a = 1 - \frac{1}{Z} \cdot \frac{H_{al}}{H} \cdot \frac{H}{C} \quad ,$$

Z being the composition of the aliphatic group (H_{al}/C_{al}). If only CH_3 groups are present (Z = 3), $f_a = 0.96$; for CH_2 groups, $f_a = 0.94$ and, for the very improbable case of only aliphatic CH groups, $f_a = 0.88$.

A further structural parameter is the "aromatic substitution index", S_{ar}, which gives the ratio of all C_{ar} atoms without hydrogen to the total number of C_{ar} atoms: [5]

$$S_{ar} = \frac{C_{ar\,(subst)} + C_{ar(fused)}}{C_{ar}} = 1 - \frac{H_{ar}}{H} \cdot \frac{H}{C} \cdot \frac{1}{f_a} \quad .$$

S_{ar} lies between 0.37 and 0.42 for the γ-fraction, depending on the value chosen for f_a. For a mean cluster with 3-4 condensed rings, there is approximately one substitution per cluster; if there are 4-5 condensed rings per cluster, only one substitution per two clusters would be present.

From the positions of the aliphatic CH-stretching bands one can conclude that CH_2 groups and/or CH_3 groups directly attached to aromatic rings are present. Since it follows from the f_a-value that there is only one C_{al} atom per 19 C_{ar} atoms, it can reasonably be assumed that all aliphatic groups are directly linked to the aromatic clusters. This fact allows the calculation of the ratio H_{ar}/C_{ar} of the unsubstituted aromatic hydrocarbon: [6]

$$\frac{H_{ar}}{C_{ar}} = \left(\frac{H_{ar}}{H} + \frac{1}{2} \frac{H_{al}}{H} \right) \cdot \frac{H}{C} \cdot \frac{1}{0.94} = 0.653$$

for the case of CH_2 groups only, or

$$\frac{H_{ar}}{C_{ar}} = \left(\frac{H_{ar}}{H} + \frac{1}{3} \frac{H_{al}}{H} \right) \cdot \frac{H}{C} \cdot \frac{1}{0.96} = 0.618$$

if only CH_3 groups are present.

If the molecules in the γ-fraction contain only one aromatic cluster, its size should be 4-5 aromatic rings. This value is somewhat higher than that which has been estimated from H/C alone, because in the latter case, the γ-fraction was assumed to be completely aromatic ($f_a = 1$). Since the molecular weight of aromatics with $R_{ar} = 4\text{-}5$ is 255 ± 40, whereas the experimentally determined mean molecular weight is 305 ± 20, the possibility exists that some molecules contain more than one aromatic cluster. Examples which would give the right H_{ar}/C_{ar} value but have a somewhat higher molecular weight include the dimers of phenanthrene and anthracene ($H_{ar}/C_{ar} = 0.643$, M = 354).

3) From the intensities and positions of the aromatic C=C stretching bands between 6 and 7 μ (1665-1430 cm^{-1}), it can be concluded that only small amounts of benzene rings are present.

4) Finally, a qualitative interpretation of the infrared absorption bands between 11 and 14.5 μ (910-690 cm^{-1}) can be made. The strongest and broadest absorption occurs between 12.6 and 13.9 μ (795-720 cm^{-1}) and can be assigned to aromatic HCC rocking vibrations, whereby 3 and 4 aromatic hydrogen atoms are adjacent to each other. The two somewhat weaker bands between 11.7 and 12.6 μ (855-795 cm^{-1}) belong to the same type of vibrations, but have to be assigned to single and two adjacent hydrogen atoms.

The γ-fraction was analyzed quantitatively by vapor phase chromatography (VPC) with linear temperature programming from 75° to 375°C on a column consisting of 25 per cent silicone gum rubber on chromosorb; this allowed recording of 12 well-resolved peaks. The material eluted up to 375°C corresponded to ⅔ of the total γ-fraction. The compounds corresponding to each peak were isolated and their UV spectra were taken for identification purpose. The assignment of the peaks was confirmed by isolation of larger quantities of each substance, purification and melting point determination. Results are:

Peak No.	Assignment	% in γ-fraction
1	acenaphthene	1.3
2	fluorene	0.4
3	phenanthrene anthracene	5.2
4	mixed methyl-phenanthrenes	1.3
5	fluoranthene	6.5
6	pyrene	5.7
7	1, 2-benzanthracene	3.0
8	chrysene	11.7
9	benzopyrenes	15.7
10	3, 4, 9, 10-dibenzopyrene	6.5
11	?	4.4
12	?	1.3

Furthermore, in separate runs, benzofluoranthenes, dibenzofluoranthenes, and 1, 12-benzoperylene have been identified qualitatively. Finally, two more polycyclics have been isolated qualitatively from the γ-fraction by adsorption chromatography; they are picene and coronene.

The above results indicate that the amount of alkylated structures present in the eluted part of the γ-fraction is low. On the other hand, the identified substances show an increasing number of condensed aromatic rings but with a mean aromatic cluster size $\bar{R}_{ar}$ = 4-5.

The question remains whether 37 per cent of the γ-fraction, which could not be determined by VPC, consists of molecules with still larger clusters or of molecules which possess more than one aromatic cluster. The answer seems to be established by the fact that the UV absorption spectrum of a mixture of the compounds found by VPC in their true concentrations is fairly similar to that of the γ-fraction itself. This observation is a strong indication that the part undetected by VPC should consist of aromatic systems of essentially the same aromatic cluster size as that found for the detected 63 per cent but linked together to form bigger molecules. This conclusion is further supported by the solubility of the γ-fraction in pet. ether, because dimers or even trimers are more soluble than molecules having the same number of rings but all condensed to one single cluster.

6. STRUCTURAL INVESTIGATIONS OF THE β-FRACTION

In the preceding pages, only the two fractions (α and γ) with extreme solubility characteristics and with certainly the biggest difference in molecular weights have been discussed. The β-fraction can be considered as intermediate; since this fraction amounts to 44 per cent of Pitch No. 5, establishment of its mean structure appears necessary.

It was necessary to determine whether the molecules in the β-fraction consist of only one aromatic cluster, in which case the cluster size should be between that of the γ-fraction and the α-fraction, or whether the molecules in the β-fraction contain more than one aromatic cluster, in which case the cluster size may be the same as in the γ-fraction, but the degree of polymerization higher. If the γ- and α-fractions are compared with the benzene extract, it can be seen that there is considerable evidence against the first hypothesis: i) the atomic H/C ratio of the benzene soluble extract is 0.617 (γ-fraction: H/C = 0.674; α-fraction: H/C = 0.384), ii) the volatile matter is 84.6 per cent (γ-fraction: 99.2 per cent; α-fraction: 13.6 per cent), and iii) the reconstruction of the UV spectrum with the help of nine model compounds [7] leads to $\bar{R}_{ar} \simeq 4$ (γ-fraction: $\bar{R}_{ar} \simeq 3$-4; α-fraction: not measured for reasons of insolubility, but certainly a much higher $\bar{R}_{ar}$ value) thus, indicating that the size of the clusters in the benzene soluble extract should be much more similar to that in the γ-fraction than that in the α-fraction. Since the β-fraction represents ⅔ of the benzene soluble extract, the mean cluster size in the β-fraction cannot be dissimilar. The fact that the β-fraction is insoluble in pet. ether, whereas the γ-fraction is soluble, can thus best be explained by a difference in molecular weight. Therefore, the second hypothesis is the more probable one (mean cluster size in the β-fraction similar to that in the γ-fraction, but a higher degree of polymerization).

The infrared spectrum of the benzene soluble extract is in its pattern more or less the same as that of the γ-fraction (see Figure 1) and of the β-fraction (see Figure 4). On the other hand, the infrared spectrum of the α-fraction shows no sharp specific bands at all and is in its aspect comparable to that of highly cross-linked or polymerized materials.

An investigation was undertaken to find a suitable method for a stepwise precipitation of the benzene soluble, but pet. ether insoluble fraction from a pyridine solution. From a great number of preliminary experiments, the following procedure was found to be the best: From the pyridine solution, about 50 per cent can be precipitated with increasing amounts of pet. ether (30/40°C); further precipitation occurred only when pyridine was progressively washed out with water from the pyridine/pet. ether solution. Finally, the last 20 per cent of the starting material has been recovered by evaporation of the solvent mixture. Altogether, 17 subfractions have been collected. The mean molecular weight has been determined for each of these subfractions and their UV, visible, and infrared absorption recorded.

The molecular-weight determination has been carried out with the help of the Hill-Baldes method, [8] which is based on the vapor pressure depression of

the solvent by the dissolved material. Since the fractions are easily soluble in pyridine and since a true chemical solution is present, the error in the molecular-weight determination should not be higher than ± 5 per cent. However, it should be remembered that this method yields number average molecular weights. Errors in molecular weight, due to association, as reported recently in the literature, can be excluded when pyridine is used as a solvent. Several mixtures of quinones and phenols including quinhydrone have been investigated in this laboratory by the method used for pitch fractions and the correct molecular weight has been found.

Figure 2 shows that the molecular weight distribution is not a smooth one; there are sharp steps between $\bar{M} = 1100 \pm 100$, $\bar{M} = 550 \pm 50$ and $\bar{M} = 280 \pm 30$.

From each of the three groups of materials, one typical sample has been chosen (further on called β_{300}, β_{600} and β_{1100}) for careful analysis.

Elementary analyses have been carried out, helium densities determined and aromaticity values calculated with the help of the graphical densimetric method.

Elementary analyses of the three subfractions are comparable (see Table 4). If the total number of C atoms per molecule is calculated and these values are converted into the number of condensed aromatic rings in one cluster (taking into account an average type of condensation, peri as well as angular), the resulting values for R_{ar} are 6, 13, and 23 in β_{300}, β_{600}, and β_{1100}, respectively. The good solubility of the subfractions in pyridine and even in benzene is in complete contradiction with such R_{ar} values of β_{600} and β_{1100}. Furthermore, the large increase in cluster size (6 → 23) would demand a much greater decrease in hydrogen content than has been found experimentally, but the existing small decrease can be easily explained by an increasing degree of polymerization.

Finally, the softening points which have been measured with a hot-stage microscope are in complete disagreement with the high R_{ar} values in β_{600} and β_{1000}. On the other hand, the trend in the increase of the softening points, which is comparable to that of naphthalene → dinaphthyl, or that of dimethylnaphthalene polymerized with formaldehyde to its dimer and trimer, is a further strong indication for the polymeric character of β_{600} and β_{1100}.

The density values show a remarkable increase from β_{300} to β_{600} and β_{1100}. If only one cluster per molecule is present, an explanation would be that the cluster size increases considerably from β_{300} to β_{600}, but changes only slightly from β_{600} to β_{1100}. This supposition is in accord with the observed trend of the H/C ratios, but the decrease of the H/C ratio, from β_{300} to β_{600} is too small to account for the large increase in density. Furthermore, it is not possible to correlate an approximately equal size of clusters in β_{600} and β_{1100} with the observed increase of the molecular weight. The above interpretation of the density values is based on the assumption that all three samples possess the same state of aggregation.

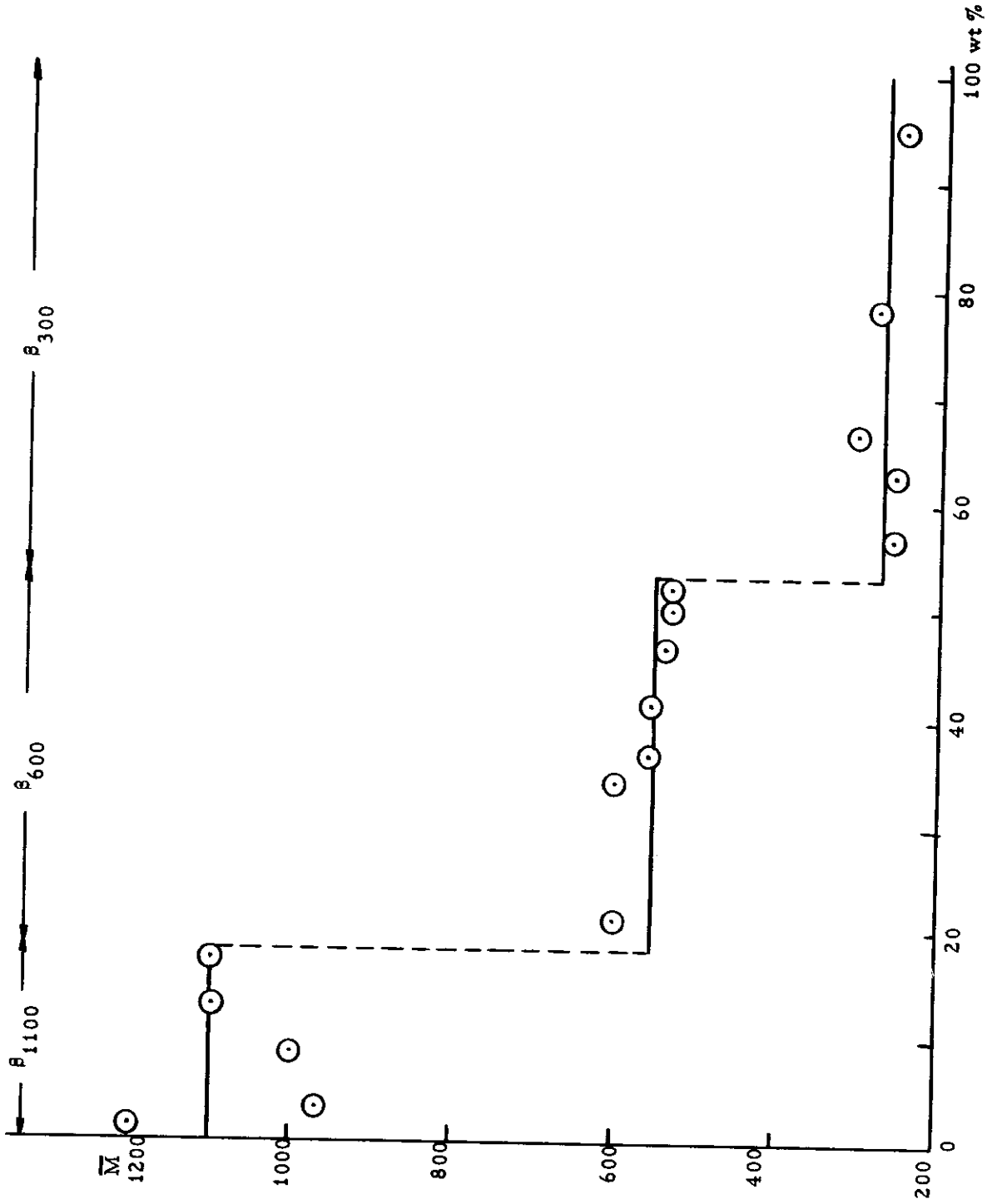

Figure 2. Molecular Weight Distribution of the β-Fraction

Table 4. Analytical Data, Helium Densities and Aromaticity Values from Graphical Densimetric Method of the Three Typical Subfractions

	β_{300}	β_{600}	β_{1100}
% C	90.2	90.0	89.8
% H	4.6	4.3	4.1
% O	2.0	2.0	2.3
% $(N + S)_{diff}$	3.2	3.7	3.8
H/C	0.608	0.569	0.544
% ash	----	----	~ 1.0
softening point (°C)	75	155	205
d_{He}^{25}	1.3116	1.3920	1.400
f_a	0.95	0.89	0.89
$\bar{R}_{ar}$(UV)	3.9	4.4	4.7

Commenting on aromaticity values obtained with the help of the graphical densimetric method [9] the true aromaticity value can be derived by this method only when i) the state of aggregation, ii) the type of condensation, and iii) the number of clusters per molecule are known [10] in addition to elementary analysis and true density. Recent investigations on a few model compounds have shown that point (iii) does not influence the f_a value as long as the cluster size is relatively small and the degree of polymerization low (dimers, trimers). Since the X-ray pattern of Pitch No. 5 is typical for an amorphous material [11], the same state of aggregation is believed present in the three subfractions β_{300}, β_{600} and β_{1100}. Although there are no experimental results available to characterize the type of condensation in the clusters, peri-condensation is believed to be the favored type. Therefore, the f_a values reported in Table 4 are based on i) amorphous state of aggregation, ii) peri-condensed clusters, and iii) one cluster per molecule. Any contribution of angular condensed clusters would increase the reported f_a values somewhat.

The UV and visible absorption spectra of the 14 subfractions fall also into three groups according to the results of the molecular weight distribution. Figure 3 shows the light absorption between 320 and 600 mμ of 3 typical subfractions in pyridine; K values decrease with decreasing $\bar{M}$, especially above 350 mμ. If only aromatic hydrocarbons with one cluster per molecule were present, this absorption behavior means that the cluster size would increase somewhat with increasing $\bar{M}$.

With the help of a reconstruction method [7], it is possible to determine from the UV and visible absorption spectrum the mean cluster size ($\bar{R}_{ar(UV)}$). The results show definitely that such small $\bar{R}_{ar}$ values can only be correlated

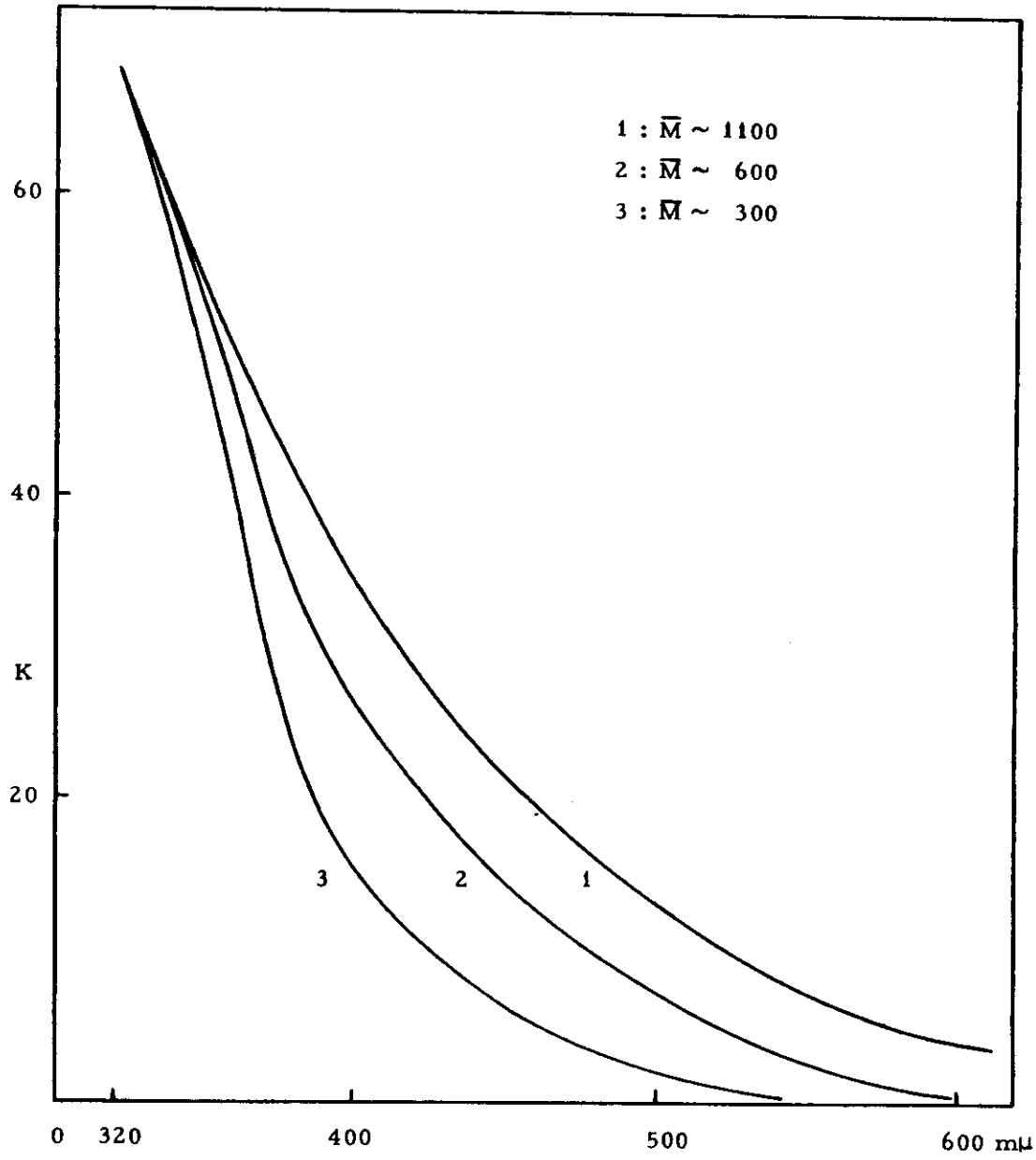

Figure 3. Light Absorption of Three Typical Subfractions

with the corresponding $\bar{M}$ if more than one aromatic cluster per mean molecule is present.

The small increase of $\bar{R}_{ar}$ ($\beta_{300} \rightarrow \beta_{1100}$) can be explained by the fact that for the reconstruction of the light absorption, only condensed aromatic hydrocarbons with one cluster per molecule have been used, and that the polymeric character of the sample has thus been neglected. However, direct bonds between aromatic systems are known to produce red shifts, which show up as an increase in $\bar{R}_{ar}$ as determined by the reconstruction method (for example 2-2' dinaphthyl : theoretically $\bar{R}_{ar(UV)}$ should be 2, but from the reconstruction of the spectrum follows ~ 3). Therefore, the mean aromatic cluster size can be the same in all three subfractions and even somewhat smaller than the values given in Table 4.

A further strong evidence for a relatively small mean cluster size in all three subfractions follows from the additional light absorption in conc. H_2SO_4 [12]. The H_2SO_4 solutions of the three samples show, in comparison with solutions in common organic solvents, strong additional absorption bands in the visible region. This effect is due to carbonium- and/or positive radical-ion formation. The wavelength region and the intensity of the additional absorption in H_2SO_4 depends mainly on the aromatic cluster size and the type of condensation [12]. In β_{300}, β_{600} and β_{1100} the maximum of the additional absorption, with practically the same intensity, occurs at 530, 610 and 630 mμ, respectively. These results indicate that the mean cluster size in β_{600} should be somewhat bigger than in β_{300}, whereas in β_{600} and β_{1100} the cluster size should be very similar. From a graph of the position of the maximum for the additional absorption versus the number of condensed aromatic rings of model compounds, $\bar{R}_{ar}$ should be 4-5, 6 and 6-7 in β_{300}, β_{600} and β_{1100}, respectively, if only one cluster per molecule is present. However, the additional absorption band shows a red shift as soon as direct bonds between aromatic clusters are present (anthracene: additional absorption at ~ 410 mμ; dianthryl: at about 480 mμ). Taking this fact into account, the $\bar{R}_{ar(UV)}$ values found are in agreement with those estimated from the position of the additional absorption in conc. sulfuric acid.

The infrared spectra (5.5-15 μ) of the same three subfractions, which are typical examples for the molecular weight distribution, show no important differences (see Figure 4), indicating that all structural features which are characterized by the infrared bands are very similar in the three subfractions.

An important parameter for the explanation of the structure is the hydrogen distribution (H_{ar}/H_{al}), which can be obtained from quantitative infrared absorption measurements in the CH-stretching region [4,5]. Following the same procedure as described in Section 5, H_{ar}/H_{al} was found to be 6.5, 5.8 and 8.0 for β_{300}, β_{600}, and β_{1100}, respectively. With the help of the total hydrogen content from elementary analysis, H_{ar}/H can be calculated and lies between 0.85 and 0.90 in the three samples. The result for β_{300} may be less accurate than the two other values because the CH-stretching absorption is overlapped by a broad absorption starting at about 2.85 μ (3510 cm^{-1}). Since this broad absorption, which could be assigned to OH- and/or NH-groups, is present mainly in β_{300}, this fraction should contain the major part of these functional

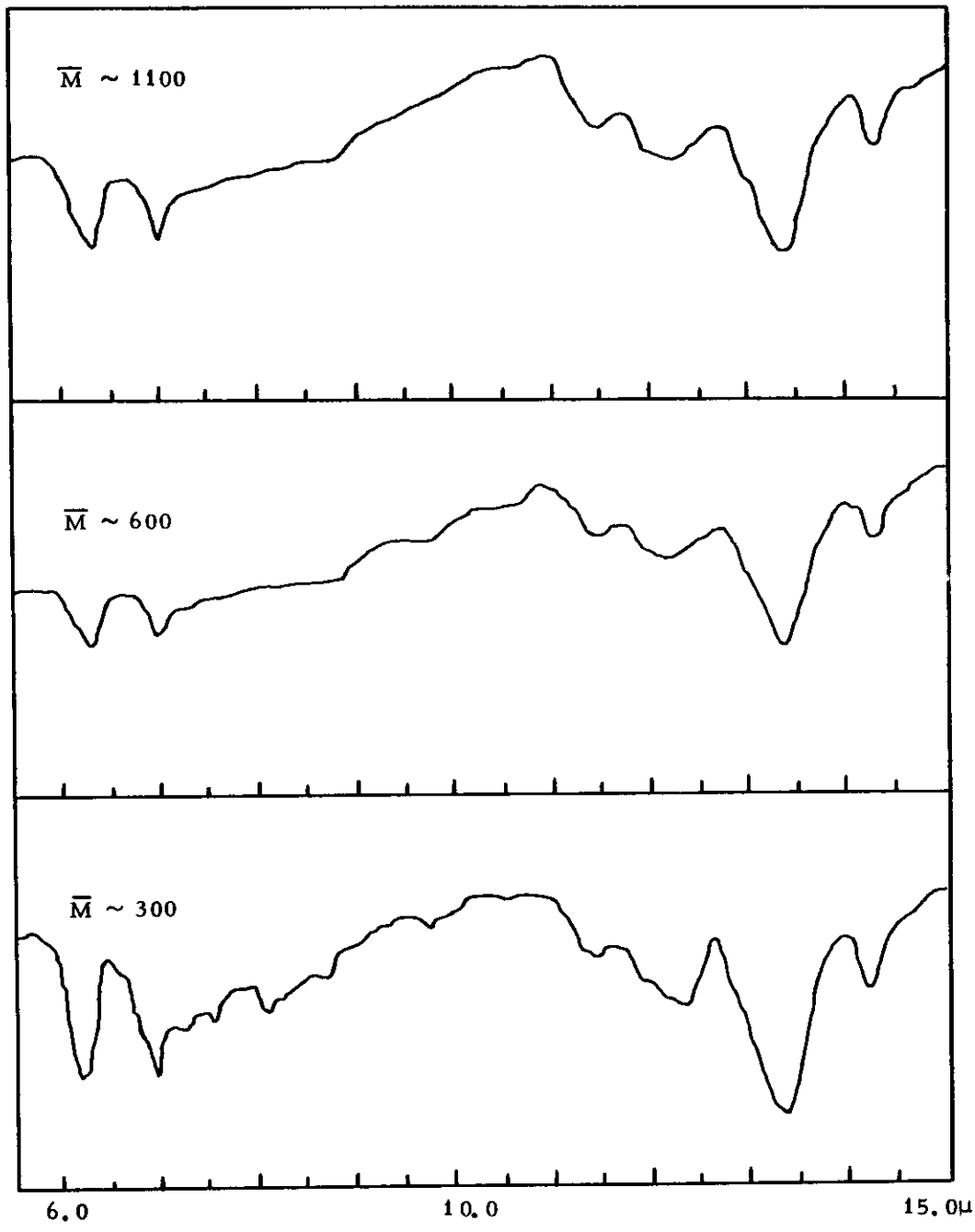

Figure 4. Infrared Absorption Spectra of Three Typical Subfractions

groups. The hydrogen distribution has also been established by proton spin resonance spectroscopy (PSR). For these measurements the samples have been dissolved in deuterated pyridine. Whereas β_{300} and β_{600} are sufficiently soluble for an exact determination of the hydrogen distribution, this behavior is not the case with β_{1100} and therefore the spectrum in Figure 5 is represented by a broken line. A comparison of all three spectra shows that mainly aromatic protons (peak at 7.5) are present and that these peaks are well separated from the three weak peaks (at 3.5, 2.3 and 1.2) which can be assigned to aliphatic protons. (In the case of β_{300} the aliphatic peaks are increased by a factor of 5 as against the aromatic peak.)

Table 5 gives the ratio $(H_{ar} + H_{OH})/H$ from PSR and shows the correctness of the parameter H_{ar}/H obtained by infrared spectroscopy.

Table 5. Structural Parameters Derived from Hydrogen Distribution and Elementary Analysis

Structural Parameter		β_{300}	β_{600}	β_{1100}
$(H_{ar} + H_{OH})/H$	(PSR)	0.87	0.87	(0.90 - 0.95)
H_{ar}/H	(IR)	0.87	0.85	0.90
H_{al}/H	(PSR)	0.13	0.13	(0.10 - 0.05)
$H_{al(\alpha C)}/H_{al(rest)}$	(PSR)	~ 7	~ 3	(~ 3)
$f_{a(CH_3)} = f_{a(max)}$		0.97	0.97	(0.98)
$f_{a(CH_2)}$		0.96	0.96	(0.97)
$f_{a(CH)}$		0.92	0.93	(0.94)
$\bar{S}_{ar}$		0.45	0.50	0.49
H_{ar}/C_{ar}		0.59	0.53	0.52
$\bar{C}_{ar(subst)}$/ molecule		1.2	4	6 - 8
$\bar{C}_{ar(subst)}$/cluster		1.2	2	2; 1.5 - 2

Chemical shift measurements ($Si(CH_3)_4$ as internal standard) show that two of the three aliphatic peaks, those at 3.5 and 2.3, originate from aliphatic protons on saturated carbon atoms adjacent to aromatic rings ($H_{al(\alpha C)}$) and the peak at 1.2 from aliphatic protons on saturated carbon atoms further removed from aromatic rings ($H_{al(rest)}$).

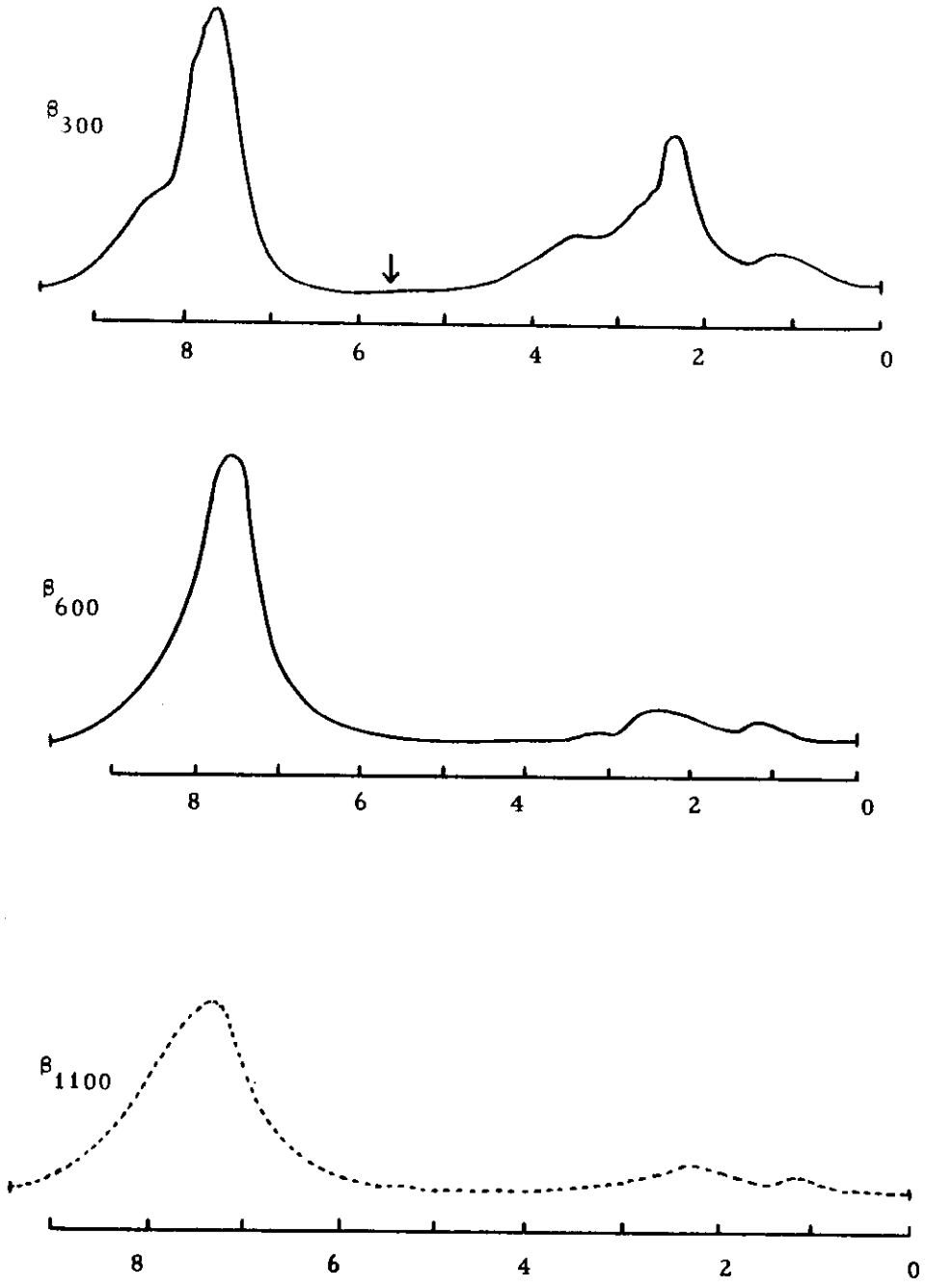

Figure 5. PSR (Proton Spin Resonance) Spectra of Three Typical Subfractions

In β_{300} and β_{600} the ratio $H_{al(\alpha C)}/H_{al(rest)}$ can be established, whereas in β_{1100} it can only be estimated. The results summarized in Table 5 show that this ratio changes definitely on going from β_{300} to β_{600}.

The aromaticity of the samples can be calculated from the hydrogen distribution in the same way as described in Section 5. Neglecting aliphatic carbon atoms with no hydrogen atoms and making the assumption that only i) CH_3, ii) CH_2, or iii) aliphatic CH groups are present, three aromaticity values can be calculated for each sample and are reported in Table 5. It is certainly not possible that only CH_3 groups are present, because there is a measurable quantity of $H_{al(rest)}$ atoms. Since it is also unrealistic to consider only aliphatic CH groups, aromaticity should best be represented by the $f_{a(CH_2)}$ values. Furthermore, the "aromatic substitution index" can be calculated (see Section 5) and the results in Table 5 show that approximately half of the aromatic carbon atoms are fused or substituted. Whatever the link between aromatic clusters may be, it is included in $\bar{S}_{ar}$ as a substitution place on each aromatic cluster. Finally, the mean composition H_{ar}/C_{ar} of the hypothetical unsubstituted aromatic hydrocarbon can be obtained (for calculation see Section 5) taking into account the measured value $H_{al(\alpha C)}/H$ and that the mean composition of the aliphatic groups directly linked to the aromatic systems is CH_2. For molecules which have more than one aromatic cluster, direct bonds and/or oxygen (sulfur) atoms which may link the clusters together are not counted as substitution places in the formula for the determination of H_{ar}/C_{ar} [6]. If the H_{ar}/C_{ar} values and the mean molecular weights of the three subfractions are compared with the theoretical possibilities, the best fit for β_{300} is obtained with one peri-condensed aromatic cluster of size $\bar{R}_{ar} = 5$, for β_{600} two such systems are linked together and in β_{1100} 3 to 4 clusters of the same size should be linked together. In the last case, 4-5 peri-condensed clusters with $\bar{R}_{ar} = 4$ are also possible. From these cluster sizes of the subfractions together with the $\bar{S}_{ar}$ values, one can deduce that the number of substituted $\bar{C}_{ar}$ atoms is distributed as follows: approximately 1 per molecule of β_{300}, 4 per mean molecule of β_{600}, and 6-8 in β_{1100}, or in <u>each cluster</u> 2 (1 cluster-cluster link, 1 substitution).

Recently, a report from C. W. DeWalt, Jr. et al. [13] on PSR measurements of coal tar pitches has come to our attention. The structural parameters calculated from hydrogen distribution, are in good agreement with the results discussed above.

7. CONCLUSIONS ON THE MOLECULAR SPECIES AND THEIR STRUCTURE IN PITCH NO. 5

From all the results, the molecular species in Pitch No. 5 can be subdivided into three groups:

a) molecules which contain only one aromatic cluster (γ-fraction; part of β_{300}),

b) aromatic clusters linked together, but with a relatively low degree of polymerization (part of β_{300}; β_{600}; β_{1100}; $(\alpha_1+\alpha_2)$), and

c) highly cross-linked aromatic systems and very big aromatic clusters (α_3-fraction).

Aliphatic substitution must be very low for all molecular species, and the mean cluster size increases somewhat on going from the γ-fraction to the $(\alpha_1 + \alpha_2)$-fraction (which is still soluble in pyridine). Each group of different molecular species will show different behavior on carbonization. Molecular species of group (a) will in part evaporate, in part polymerize and condense. Molecular species of group (b) will evaporate only to a small extent, and, being more stable than the compounds of group (a), will become reactive at a later stage of carbonization. Finally, molecular species of group (c) are believed to be very unreactive.

This interpretation suggests that the quality of a pitch as a binder depends strongly on the chemical reactivity of the molecular species of groups (a) and (b), a hypothesis supported by the following investigations of J. C. Pariaud [2]. Pitches were extracted with pyridine (pyridine insoluble residue = part C) and the extracts precipitated with water in two steps (parts A and B, see Section 3). The same pitches were heated up to 400°C and the same extraction and precipitation procedure was performed on these samples as on the original pitches. Without any structural investigations, Pariaud found two classes of pitches:

1) those in which part C remains practically constant and the amount of part A increases at the expense of part B, and,

2) those in which part C increases considerably whereas part A and B decrease.

From graphitization experiments, Pariaud concluded that the quality of a pitch is related to the classification defined above.

Since part B in its structural features should be comparable with the γ-fraction, part A with the β- and $(\alpha_1 + \alpha_2)$-fraction and part C with the α_3-fraction, it is necessary to investigate the changes of physical properties and structural parameters of Pitch No. 5 and its fractions with increasing temperature.

8. THE PLASTIC BEHAVIOR OF PITCH NO. 5, ITS EXTRACTS, AND ITS FRACTIONS

One of the most sensitive physical properties on which to observe polymerization and condensation reactions is the viscosity. Additional important information can be gained by measuring the temperature dependence of the viscosity and the changes of the viscosity at a given temperature with time. Finally, one has to investigate whether the viscosity depends on the controlled atmosphere (N_2, air, O_2) under which the heat-treatment is carried out.

Since the viscosity of pitches at the softening point is of the order of 10^6 cS (centistokes) but diminishes tremendously with increasing temperature (an increase of 60°C corresponds to a decrease of the viscosity by a factor of 1000), the Gieseler-Hoehne plastometer [14] has been chosen for the determination of the plastic behavior of the samples under investigation.

The standard conditions established are as follows:

1) amount of sample : 2 g
2) particle size : ~ 1 mm
3) load : 10 g
4) heating rate : 3°C/min
5) rate of gas flow : 10-20 cm^3/min - starting half an hour before heating.

The plasticity values are expressed in the number of revolutions of the stirrer per minute (rev/min). As soon as the number of revolutions becomes about 1000, results get uncertain and measurements have, therefore, been stopped at that temperature at which 1000 rev/min have been reached. Furthermore, the softening point as measured by the plastometer has been defined as the temperature at which the number of rev/min is 0.1 (36 angle degrees). Finally, the correlation of the number of rev/min with absolute value of the kinematic viscosity has been determined. Taking into account the standard experimental conditions, it is found that $\eta_k = 10^6/2$ (rev/min).

8.1. Plastic Behavior of Pitch No. 5

From the various runs up to 165°C (Figure 6), the following conclusions can be drawn:

i) if the powdered pitch sample is at first heated up to 165°C under nitrogen (Figure 6 a), under air or oxygen (Figure 6 b), cooled down to room temperature in the plastometer and then heated up again to the same temperature, no change in the plasticity and its temperature dependence is observed;

ii) measurements at 150°C and 165°C show that the plasticity is independent of the time of heat-treatment and of the controlled atmospheres used (N_2, air, O_2).

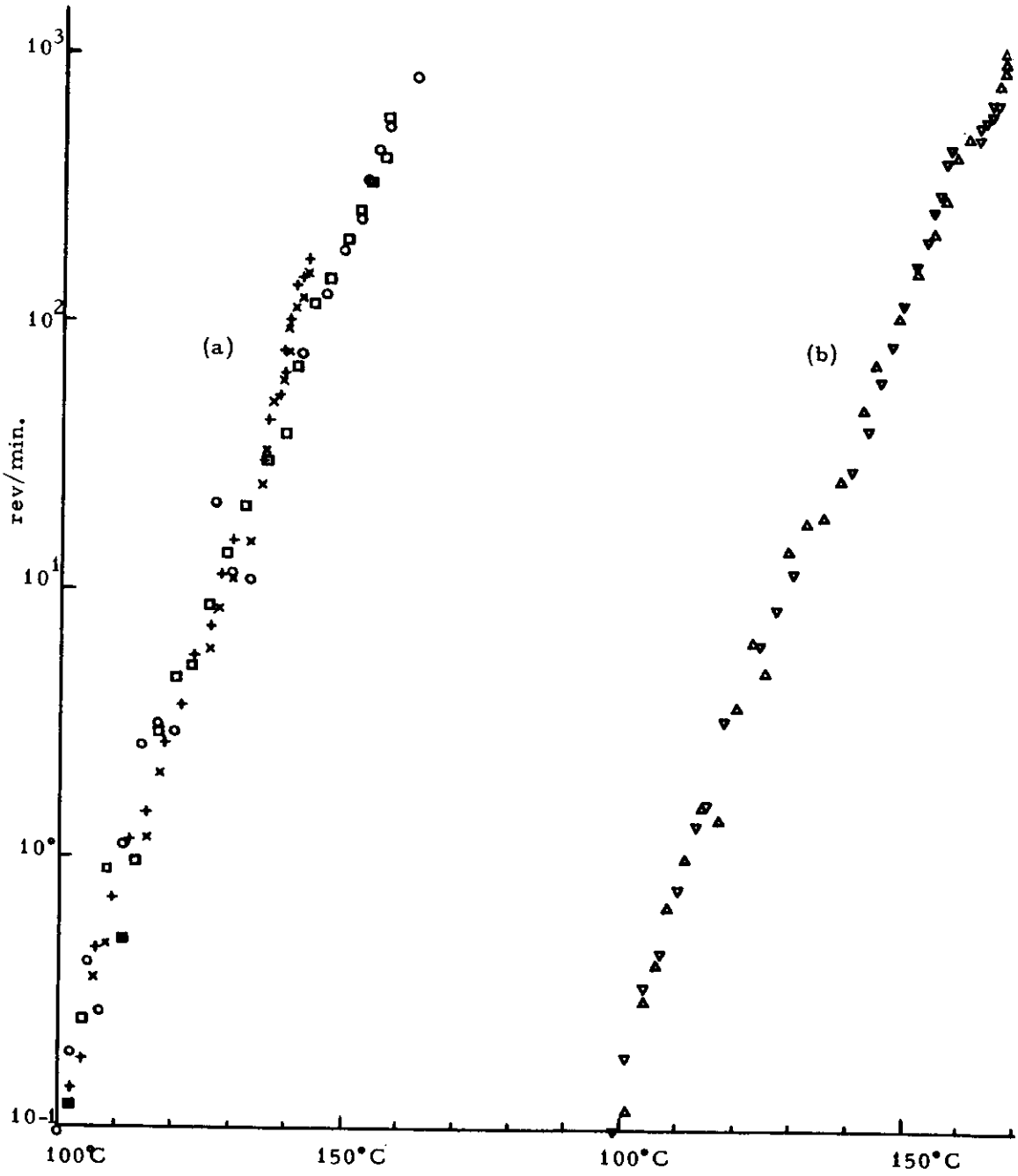

(a) Experiments carried out under N_2; fresh samples (O; +) second runs (□ ; X)

(b) Experiments carried out under air (△) or under oxygen (▽)

Figure 6. Changes of Plasticity of Pitch No. 5 with Temperature up to 165°C

To establish any structural changes up to 190°C and 220°C, at which temperatures the plasticity can no longer be measured with the Gieseler-Hoehne plastometer (rev/min>> 1000), the following indirect way has been chosen: the sample is heated in the equipment to 190°C or 220°C, but the plastic behavior is measured only to about 165°C. When the temperature of 190°C or 220°C is reached, it is held constant for 80-90 minutes, the sample is then cooled to room temperature and the plasticity measured again to 165°C ("second run").

Figure 7 shows no significant changes when the experiments have been carried out under nitrogen (the full line represents the mean temperature dependence of the plasticity from Figure 6). Parallel investigations under air or pure oxygen have also been carried out. Figure 8 shows that the plasticity decreases significantly after prolonged heat-treatment at 190°C. This effect is certainly much more pronounced in oxygen than in air (in oxygen the number of rev/min decreases by a factor of 7-8 after the single heat-treatment, whereas under air this decrease is only observed after three heat-treatments).

Figure 9 summarizes all results for 220°C under air or oxygen and shows that a short heat-treatment (40 min) under air does not produce a remarkable change in plasticity. On the other hand, prolonged heat-treatments at 220°C under oxygen have a significant effect. The softening point increases by as much as 45°C and the plasticity decreases by a factor of approximately 1000.

8.2. Plastic Behavior of the Benzene Soluble Extract of Pitch No. 5

The plasticity and its temperature dependence were first measured under nitrogen. Since the softening point is about 30°C (see Figure 10), the plasticity values were measurable only up to 80°C (rev/min ~ 1000, limit for reproducible data) but the sample was heated up to 200°C, held at this temperature for 100 minutes, and then cooled to room temperature. Remeasuring the plasticity showed that the softening point of the sample had increased by 20°C, but the temperature dependence remained the same as in the first run (see Figure 10 a). The results of the third and fourth run indicate that the final stage of changes in plasticity has been reached with a softening point at 60°C and a plasticity decrease by a factor of ~ 100 as compared with the first run. This result may be due to the evaporation of some highly volatile compounds in the benzene soluble extract during heat-treatment to 200°C.

Furthermore, Figure 6 and Figure 10 show that the temperature dependence of the plasticity in pitch and its benzene soluble extract is the same.

The sample of the fourth run of Figure 10 was heat-treated three times under air, the procedure being the same as under nitrogen. As can be seen from Figure 10 b,(the full line illustrates the plastic behavior of the sample after four runs under nitrogen), there is a further increase in softening point (~ 12°C) corresponding to a decrease in plasticity by a factor ~ 10. Changing in further runs from air to oxygen produces a further parallel displacement of the plasticity curves towards higher temperatures.

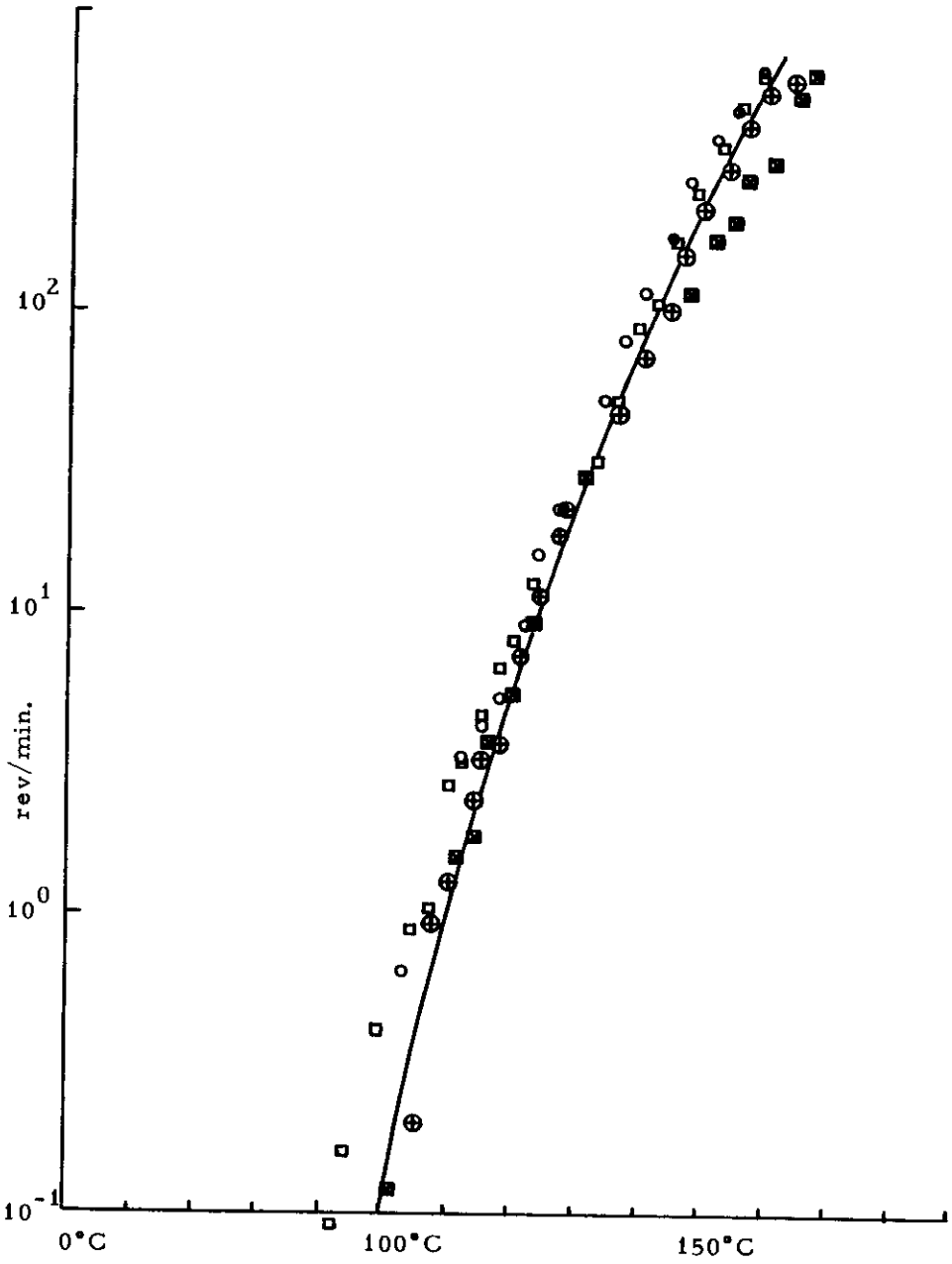

Figure 7. Changes of Plasticity of Pitch No. 5 with Temperature under N_2

Fresh sample (O) and second run (⊕); 190°C experiments.
Fresh sample (□) and second run (⊠); 220°C experiments.

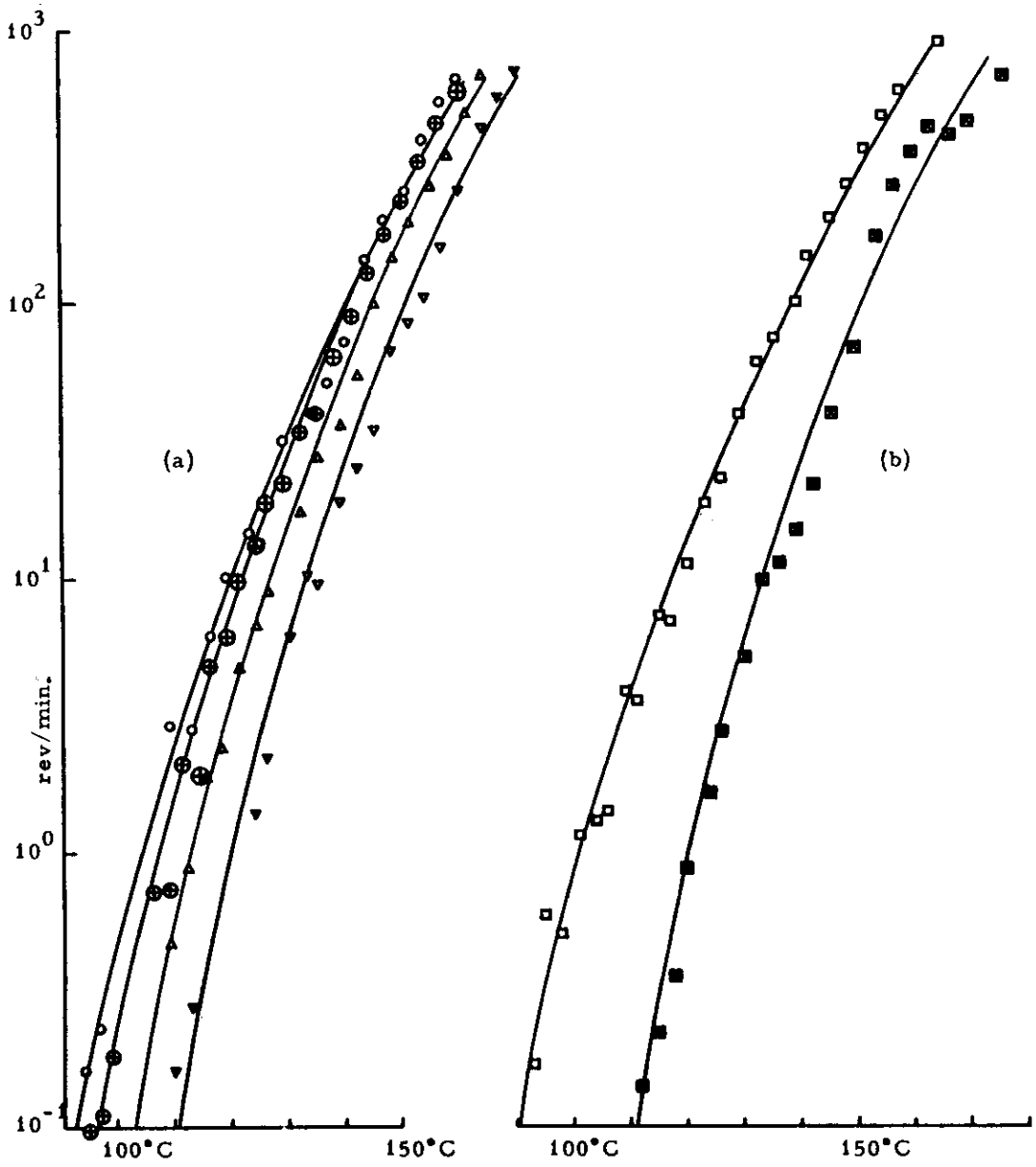

Figure 8. Time Dependence of Plasticity of Pitch No. 5 at 190°C Under Controlled Atmospheres

(a) under air: fresh sample (O) - second run (⊕); 100 min at 190°C, third run (△); 105 min at 190°C, fourth run (▽); 130 min at 190°C

(b) under oxygen: fresh sample (□) - second run (⊠); 120 min at 190°C

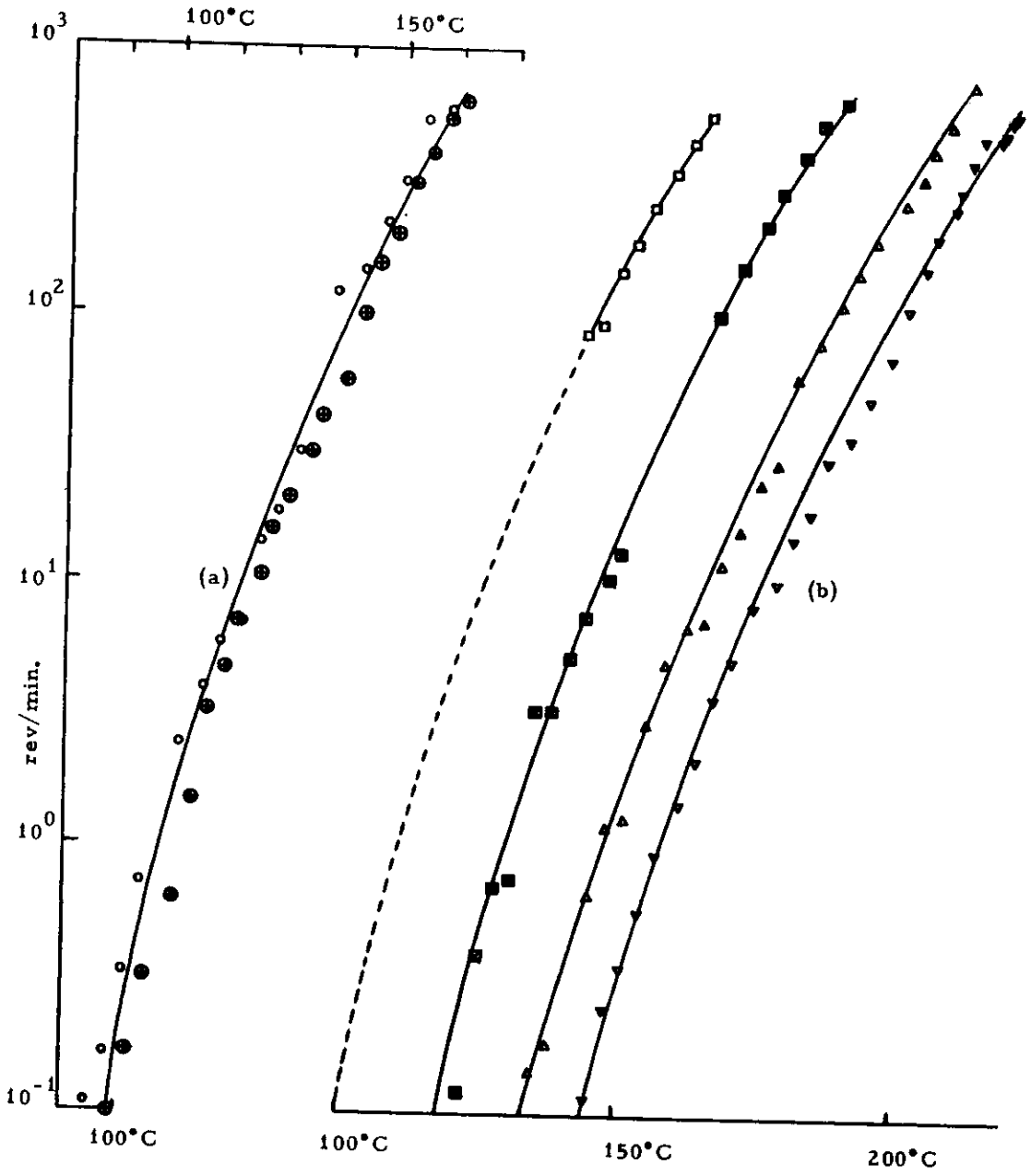

Figure 9. Time Dependence of Plasticity of Pitch No. 5 at 220°C Under Controlled Atmospheres

(a) under air: fresh sample (O) - second run (⊕); 40 min at 220°C

(b) under oxygen: fresh sample (□) - second run (⊠); 110 min at 220°C, third run (△); 100 min at 220°C, fourth run (▽); 260 min at 220°C

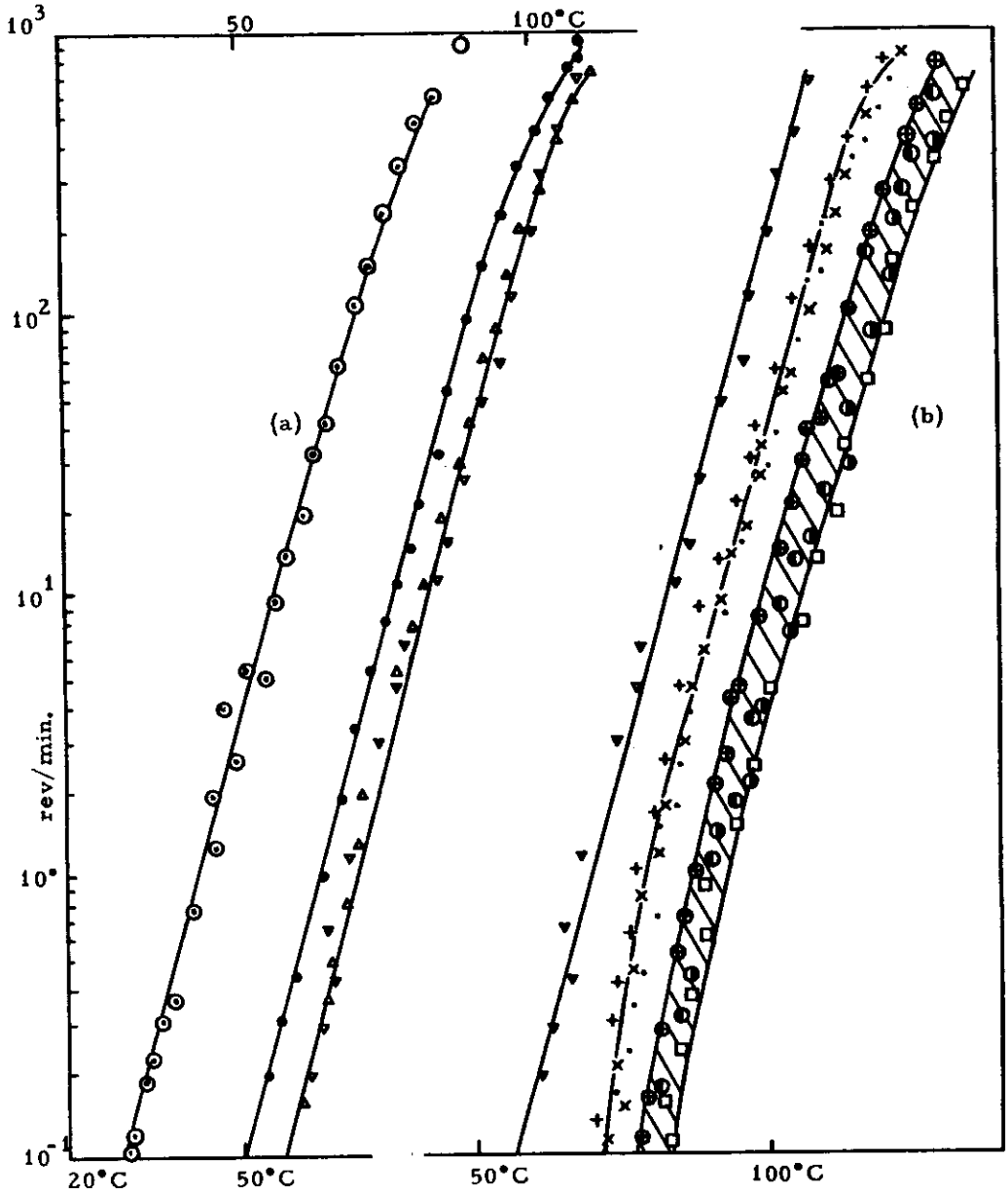

Figure 10. Time Dependence of Plasticity of the Benzene Extract of Pitch No. 5

(a) under nitrogen:

- ⊙ fresh sample
- • second run; 100 min at 200°C
- △ third run; 100 min at 200°C
- ▽ fourth run; 100 min at 200°C

(b) under air and oxygen:

- ▽ starting material = fourth run under nitrogen
- \+ fifth run; air, 100 min at 200°C
- X sixth run; " " "
- • seventh run; " " "
- ⊕ eighth run; oxygen, 100 min at 200°C
- □ ninth run; " " "
- ◐ tenth run; " " "
- ◑ eleventh run; " " "

The decrease of the plasticity under air and under oxygen, in contrast to that under nitrogen, is believed due to chemical reactions.

8.3. Plastic Behavior of the Benzene Insoluble Residue (α-fraction) of Pitch No. 5

All measurements have been carried out under nitrogen. The results are shown in Figure 11. Softening of the sample starts at about 385°C, maximum plasticity occurs at ~ 470°C and resolidification is reached at 510°C. A comparison of the plastic behavior of Pitch No. 5 and its benzene extract with that of the α-fraction shows the expected changes: i) an increase of the softening point of about 280°C and 350°C, and ii) the maximum plasticity of the α-fraction being roughly a hundred times smaller than the plasticity of Pitch No. 5 at 160°C and of the benzene extract at 80°C. It should be kept in mind that the maximum plasticities of the latter two samples are certainly much higher than the values at 160° and 80°C, respectively.

8.4. Plastic Behavior of the α_1, α_2 and α_3-Fractions of Pitch No. 5

Figure 12 includes the results on the α_1- and α_2-fractions; it can be seen that there is a certain difference between the two samples. The softening points lie between 300 and 340°C, maximum plasticity occurs in both cases at about 470°C and resolidification temperature is reached at 520-535°C. As expected, the α_1- and α_2-fractions have a lower softening point and a much higher plasticity than the α-fraction, but it is remarkable that all three fractions have practically the same temperature of maximum plasticity and of resolidification.

Finally, for the α_3-fraction, no plastic behavior could be observed at all up to 550°C.

8.5. Preliminary Conclusions Concerning the Plastic Behavior of the Molecular Species in Pitch No. 5

Although the important β-fraction has not been investigated so far, and although the complete plastic behavior (softening →maximum plasticity→ resolidification) has been measured only for a few samples, there is no doubt that a correlation exists between the plastic properties and the different molecular species.

Since the softening point of the γ-fraction is about room temperature and that of β_{300} and β_{600} ~ 55° and ~ 155°C, respectively, whereas the softening points of all other fractions are higher than 200°C, the plastic behavior of Pitch No. 5 between 160° and 180°C (temperatures at which the pitch is mixed with the coke) should depend mainly on the concentration of the γ-, β_{300}- and, to some extent, β_{600}-fraction (altogether ~ 60 per cent of the pitch). The molecular species in these fractions seem to be fairly stable, because no change of plasticity is observed, even at prolonged heating times up to 4 hours (the mixing of pitch and coke usually takes less time) and under oxygen.

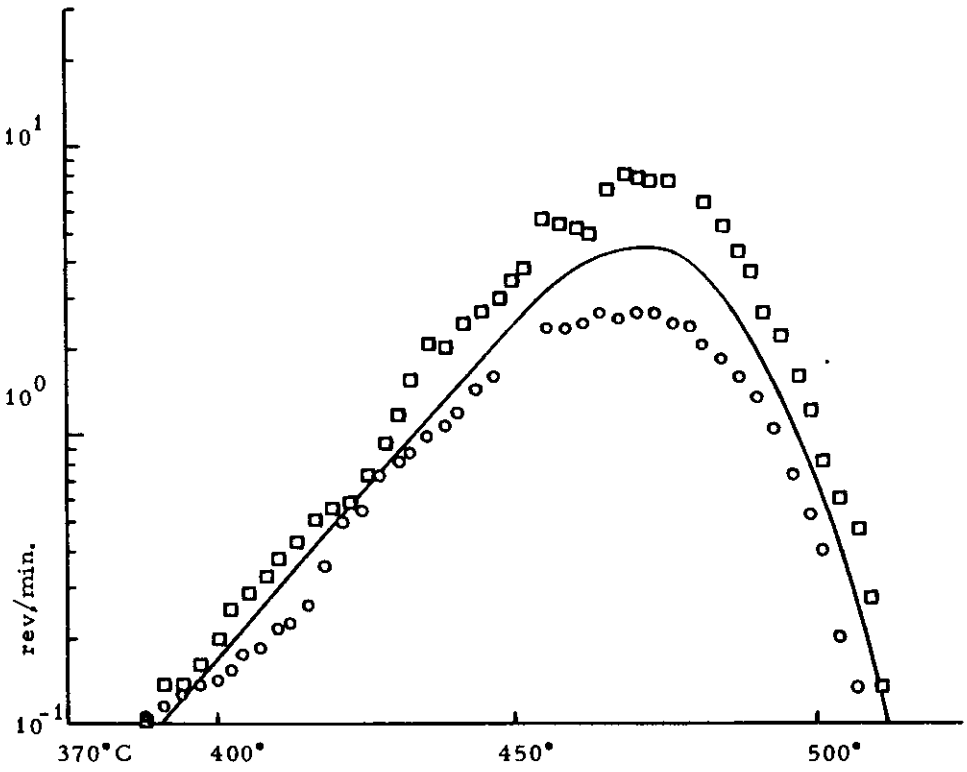

Figure 11. Changes of Plasticity of the α-Fraction of Pitch No. 5 with Temperature Under N_2

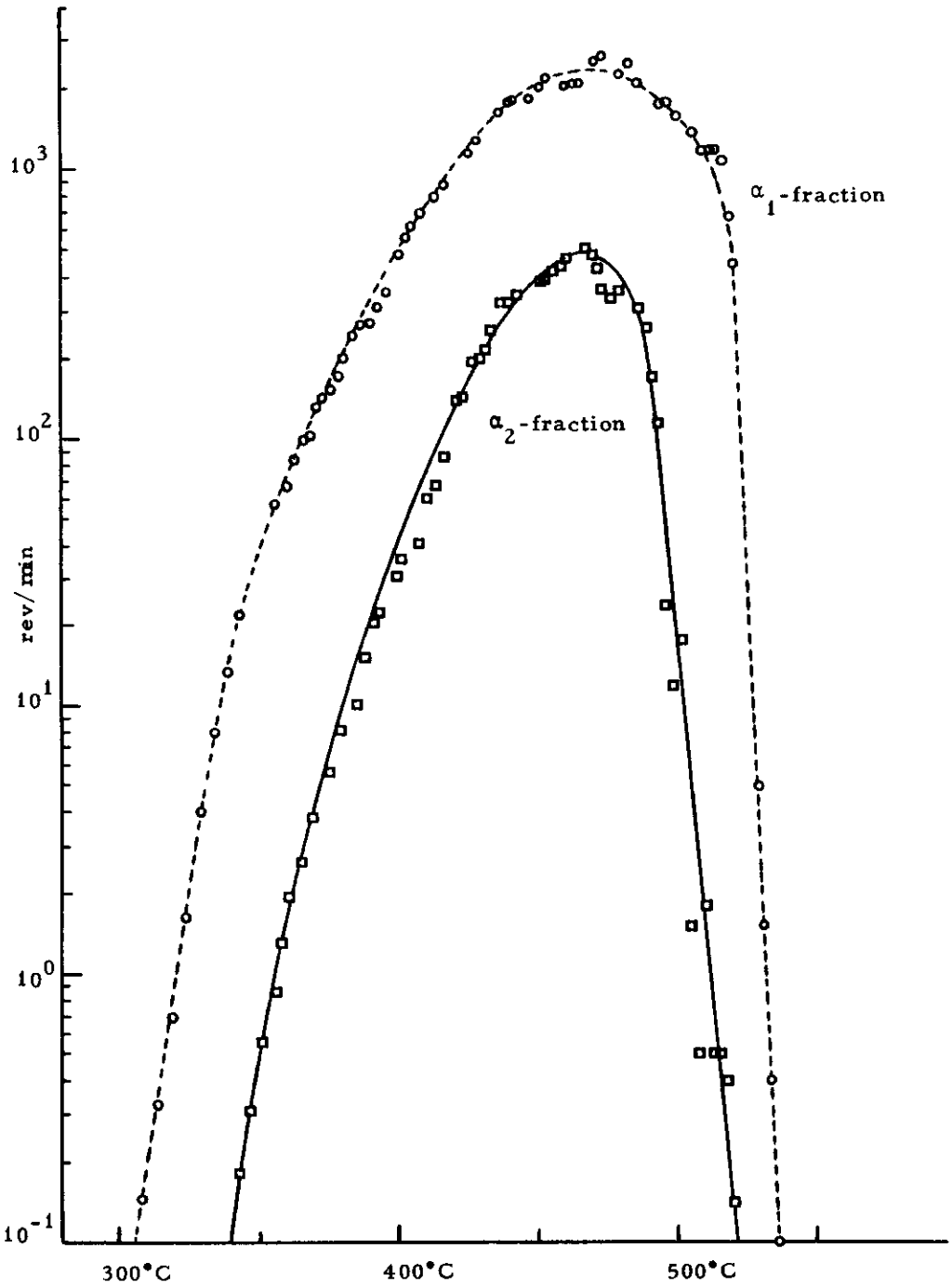

Figure 12. Changes of Plasticity of α_1-and α_2-Fraction of Pitch No. 5 with Temperature Under N_2

The behavior of pitch No. 5 up to 550°C is independent of α_3 (pyridine insoluble) but depends on chemical changes especially in the γ- , β_{300}- and β_{600}-fractions and also in the β_{1100}-, α_1 and α_2-fractions. Since these materials have their maximum plasticity at ~ 475°C, they are thought to be reactive enough for further carbonization.

These preliminary conclusions are in agreement with the interpretation of the ideas of J. C. Pariaud [2], which are based on the solubility characteristics of pitches heat-treated at 400°C, and which have already been discussed.

9. LIST OF SYMBOLS

C	:	total number of carbon atoms
C_{ar}, C_{al}	:	number of aromatic and aliphatic carbon atoms
${}^{\alpha}C$	:	number of aliphatic carbon atoms directly attached to aromatic rings
f_a	:	aromaticity (C_{ar}/C)
$f_{a(CH_3)}$, $f_{a(CH_2)}$, $f_{a(CH)}$	:	aromaticity values assuming only CH_3, CH_2 or CH groups
S_{ar}	:	aromatic substitution index; ratio of the number of substituted and fused aromatic carbon atoms to the total number of aromatic carbon atoms
$\bar{R}_{ar}$	:	mean number of condensed aromatic rings per cluster
$\bar{R}_{ar(UV)}$	:	$\bar{R}_{ar}$ derived from UV and visible absorption
H	:	total number of hydrogen atoms
H_{ar}, H_{al}	:	number of aromatic and aliphatic hydrogen atoms
H_{OH}	:	number of hydrogen atoms in hydroxyl groups
$H_{al(\alpha C)}$,	:	number of aliphatic hydrogen atoms on αC atoms
$H_{al(rest)}$	:	number of H_{al} atoms on aliphatic C atoms other than αC
D_{ar}, D_{al}	:	optical density of the aromatic and aliphatic CH-stretching band
ε_{ar}, ε_{al}	:	maximum absorption coefficients of the aromatic and aromatic CH-stretching band
K	:	specific absorption coefficient
d^{25}_{He}, $d^{25}_{H_2O}$	:	helium density and water density at 25°C
M, $\bar{M}$	:	molecular weight and mean molecular weight
$\Delta\varepsilon$	:	electron activation energy in electron volt (eV)
VM	:	volatile matter
CV	:	coking value
η_k	:	kinematic viscosity

10. LIST OF REFERENCES

1. E. de Ruiter, J. F. M. Oth, V. Sandor and H. Tschamler, WADD Technical Report 61-72, Volume XI, Characterization of Binders Used in the Fabrication of Graphite Bodies.
2. J. C. Pariaud, Goudron pour routes, No. 18, March 1961 , p. 5.
3. E. de Ruiter, R. Leutner and H. Tschamler, Rec. trav. chim. 81, 5 (1962).
4. J. F. M. Oth, E. de Ruiter, H. Tschamler, Brennstoff-Chem. 42, 378 (1961).
5. H. Tschamler and E. de Ruiter, Brennstoff-Chem. 43, 16 (1962).
6. H. Tschamler and E. de Ruiter, Brennstoff-Chem. 44 (1963) in press.
7. E. de Ruiter and H. Tschamler, Brennstoff-Chem. 39, 362 (1958).
8. E. J. Baldes, J. Sci. Inst. 11, 223 (1934).
9. D. W. Van Krevelen, H. A. G. Chermin, and I. Schuyer, Fuel 36, 313 (1957).
10. V. Sandor, E. de Ruiter and H. Tschamler, Erdöl und Kohle 15, 713 (1962).
11. L. Cartz and P. B. Hirsch, Phil. Trans. Roy. Soc. London, Ser. A, 252, 557 (1960).
12. E. de Ruiter and H. Tschamler, Brennstoff-Chem. 40, 43 (1959); Fuel 41, 491 (1962); Erdöl und Kohle 16, 193 (1963).
13. C. W. De Walt, Jr. and M. S. Morgan, Mellon Institute, Pittsburgh 13, Penn.
14. Manufactured by A. D. A. M. E. L., 4 Passage Louis Philippe, Paris (XIe).